

Optical design of the post focal relay of MAORY

Lombini M.^{*,a}, Magrin D.^b, Patti M.^a, Greggio D.^b, Cortecchia F.^a, Diolaiti E.^a, De Caprio V.^d, De Rosa A.^a, Radaelli E.^f, Riva M.^f, Ciliegi P.^a, Esposito S.^c, Feautrier P.^g, Ragazzoni R.^b

^aINAF- Osservatorio di Astrofisica e Scienza dello Spazio di Bologna, Via Gobetti 93/3, 40129 Bologna (Italy);

^bINAF-Osservatorio Astronomico di Padova, Vicolo dell'Osservatorio 5, 35122 Padova (Italy);

^cINAF- Osservatorio Astrofisico di Arcetri, Largo Enrico Fermi 5, 50125 Firenze (Italy);

^dINAF- Osservatorio Astronomico di Capodimonte, Salita Moiariello 16, 80131 Napoli (Italy);

^fINAF- Osservatorio Astronomico di Brera, Via E. Bianchi 46, 23807 Merate (Italy);

^gInstitut de Planétologie et d'Astrophysique de Grenoble, 414, Rue de la Piscine, Domaine Universitaire, 38400 St-Martin d'Hères (France)

ABSTRACT

The Multi Conjugate Adaptive Optics RelaY (MAORY) is foreseen to be installed at the straight through focus over the Nasmyth platform of the future Extremely Large Telescope (ELT). MAORY has to re-image the telescope focal plane with diffraction limited quality and low geometric distortion, over a field of view of 20 arcsec diameter, for a wavelength range between 0.8 μm and 2.4 μm . Good and uniform Strehl ratio, accomplished with high sky coverage, is required for the wide field science. Two exit ports will be fed by MAORY. The first one is for a wide field Camera that is supposed to be placed on a gravity invariant port with an unvignetted FoV of 53 arcsec x 53 arcsec where diffraction limited optical quality ($< 54\text{nm}$ RMS of wavefront error at the wavelength of 1 μm) and very low field distortion ($< 0.1\%$ RMS) must be delivered. The requirements regarding the optical quality, distortion and optical interfaces, together with the desire of reducing the number of reflecting surfaces (and consequently the thermal background), optics wavefront error (WFE), overall size, weight and possibly cost, drove the design to have 2 Deformable Mirrors (DMs) with optical power. The Post Focal Relay (PFR) is also required to split the 589 nm wavelength light of the Laser Guide Stars (LGS), used for high order wavefront sensing, by means of a dichroic that lets the light of 6 LGSs, arranged on a circle of about 90 arcsec diameter, pass through and reflects science beam. Behind the dichroic an objective creates the LGS image plane for the WFSs channel. We present in this paper the optical design and the tolerance analysis of the PFR and the objective. The tolerance analysis concerning the manufacturing and the alignment precision is also shown.

Keywords: Optical design, Adaptive Optics, Astrometry, ELT

1. INTRODUCTION

The Multi Conjugate Adaptive Optics RelaY (MAORY) [1] is foreseen to be installed at the straight through focus over the Nasmyth platform of the future Extremely Large Telescope (ELT) [2]. ELT will be the largest ground based optical-IR telescope of the world and will require, to exploit its potentialities regarding the angular resolution, the wavefront correction of the star images caused by the atmospheric turbulence. Two mirrors of ELT, named M4 and M5, will be able to correct the focal plane global tilt (M5) caused mostly by the wind shake and the fast atmospheric higher order aberrations (M4, conjugate close to the ground) while the telescope itself should control and correct some the slow aberrations introduced by the gravity. In order to achieve a high sky coverage with Adaptive Optics (AO) observations, ELT will provide up to 6 Sodium Laser Guide Stars (LGSs) [4] launched from the side of the primary mirror. Due to the tilt and focus indetermination of the LGSs [5] up to 3 Natural Guide Stars (NGS) are still required to measure these aberrations but their magnitude can be much fainter respect to the classical AO systems with only NGSs, till magnitude 18-19 instead of 14.

*matteo.lombini@inaf.it

From the Adaptive Optics (AO) point of view, MAORY must deliver a good and uniform Strehl ratio, accomplished with high sky coverage, 50% of sky coverage at the galactic pole with a Strehl ratio > 30% in K-Band. To achieve these performances, the current Phase B study [1] gives a series of requirements concerning the AO system in MAORY. The PFR optical design shall create along the optical path two clear planes where to put two DMs for the wavefront correction, to be carried out together with the telescope adaptive and field stabilization mirrors m4 and M5. The requirements regarding the optical quality, distortion and optical interfaces, together with the will of reducing the number of reflecting surfaces and consequently the thermal background, optics wavefront error (WFE), overall size, weight and possibly cost, drove the design to have DMs with optical power. The PFR is also required to split the 589 nm wavelength light of the Laser Guide Stars (LGS), used for high order wavefront sensing, from longer wavelength light used for science observation and for low order wavefront sensing by the use of Natural Guide Stars (NGS). The dichroic lets the light of 6 LGSs, arranged on a circle of about 90" diameter, pass through and reflects science beam and NGS light. Behind the dichroic, an objective creates the LGS image plane for the WFSs channel.

From the pure optical design point of view the PFR of MAORY has to re-image the telescope focal plane with diffraction limited quality and low geometric distortion, over a field of view (FoV) of 200 arcsec diameter, for a wavelength range between 0.8 μm and 2.4 μm . Two exit ports will be fed. The first one is for MICADO [2] that is supposed to be placed on a gravity invariant port at 1800m below the optical axis. An unvignetted FoV of 53" x 53" with diffraction limited optical quality (< 54nm RMS of wavefront error at the wavelength of 1 μm) and very low field distortion (< 0.1% RMS) must be delivered. The full FoV can be transmitted, by means of a deployable folding mirror after the last powered mirror, to the second exit port to feed an instrument to be defined yet. The optical interface at the exit ports, as the focal ratio, the exit pupil position and focal plane curvature have been agreed with MICADO team.

2. POST FOCAL RELAY OPTICAL DESIGN

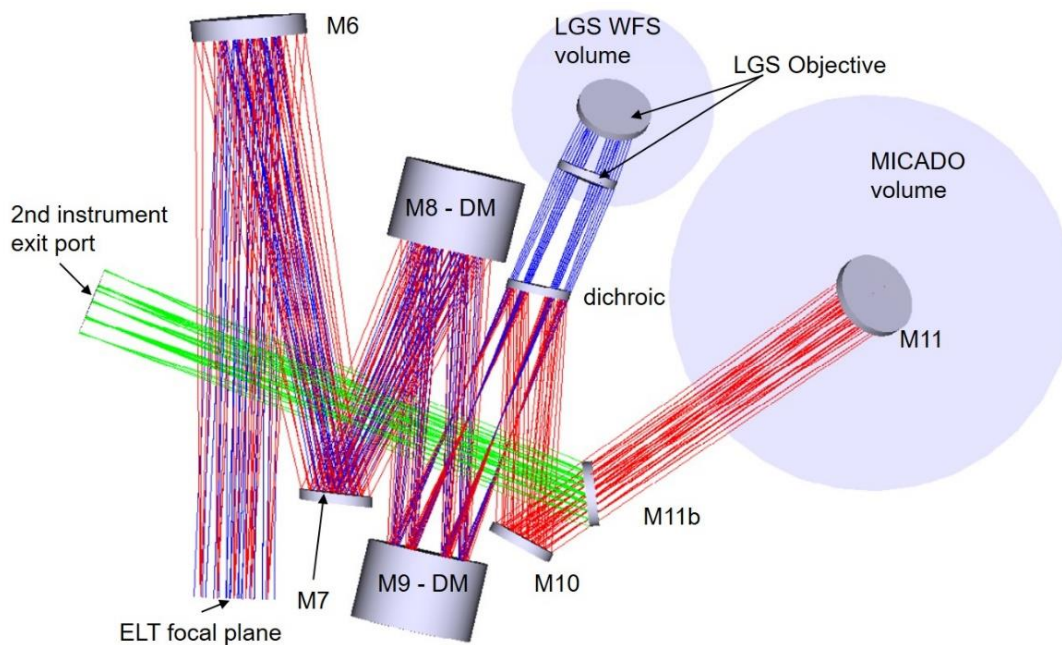


Figure 1: MAORY optical layout. Red rays: science path from telescope focal plane to MICADO. Green rays: science path to second instrument port. The M11 flat mirror to create the second port is deployable. Blue rays: LGS rays path to the WFS.

The ELT is a 5 mirrors telescope where the first 3 mirrors have optical power and the flat M4 and M5 mirrors are used to correct the wavefront aberration using the signals coming from the wavefront sensors. The baseline optical design of the Main Path Optics (MPO) of the PFR, shown in Figure 1, consists of:

- Concave off-axis mirror (M6) and convex off-axis mirror (M7), which produce a pupil image of the appropriate size (a concave mirror alone would not be enough, given the available space between the telescope focal plane and the edge of the Nasmyth platform);
- Two concave on-axis DMs (M8 and M9), with the same optical power, optically conjugated to two turbulent high altitude atmospheric layers;
- LGS Dichroic, close to the pupil image; this component is assumed to reflect the science light and transmit the LGS light;
- Convex off-axis mirror (M10), which produces the exit focal plane with the required focal ratio and exit pupil distance;
- Flat 45°-tilted mirror (M11), which folds the light to the gravity-invariant port for MICADO.
- The second instrument port is achieved by inserting a flat folding mirror (M11b) between M10 and M11.

The combination of convex mirrors (M7 and M10) and concave mirrors (M7, M8, M9) ensures flat focal surface on the exit port.

The first order parameters and the optical prescription data are listed in Table 1 and Table 2. The estimated performance and tolerance analysis are described in section 3.

Item	Value	notes
Exit focal ratio	F/17.7 (same as telescope)	same as telescope
Exit pupil distance	8000 mm (towards telescope)	towards telescope
Focal plane curvature	Flat	For AIV
NGS patrol FoV (also called technical FoV)	200 arcsec diameter	From sky coverage simulations
MICADO unvignetted FoV	Up to 75 arcsec diameter	
Transmitted wavelength range at exit port	0.6 – 2.5 μ m	Lower wavelength limit set by LGS Dichroic; higher wavelength limit set by MICADO
Post-focal DMs conjugation range	15 km, 5.5 km	From E2E calculations
Residual WFE in MICADO FoV	< 35 nm	From Error Budget
Residual WFE in the technical FoV	< 120 nm	From Error Budget
PSF Blur for single image in MICADO FoV	< 8 μ m	
Residual distortion after 4 th order transf.	< 10 μ arcsec	
Exit pupil blur in MICADO FoV	< 1/100	

Table 1. Main Path Optics general specifications.

ID	Diameter [mm]	Surface decenter [mm]	Curvature radius [mm]	Conic constant	Aspheric terms
M6	1200	340	+13000 (cv)	-1.91	
M7	750	830	+6800 (cx)	-1	
M8 – DM	890	-	+15000 (cv)	-5.13	-
M9 – DM	820	-	-15000 (cv)	2.25	-
LGS Dichroic	680	-	Infinity	-	-
M10	675	435	+53400 (cx)	0	4 th : 6.00e-13 6 th : -1.57e-19 8 th : 7.52e-26
M11	900x690	-	Infinity	-	-
* Clear aperture, M9 actual diameter will be the same as M8					

Table 2. Main Path Optics optical prescription data.

Table 2 shows the optical prescription data of the Main Path Optics. Concave surfaces are labelled as “cv” convex surfaces as “cx”. The sign convention for the radii of curvature is: positive if the centre of curvature is to the right from the surface vertex, negative if the centre of curvature is to the left of the surface vertex.

Mirrors M8 and M9 are described here as two rigid mirrors, but they are actually the two DMs in the PFR. They have identical curvature radius and slightly different conic constant. The slight difference in optical shape, as well as the deviation from the best fit sphere, is in the order of only 2-3 μm peak-to-valley and may be probably applied by active deformation of the surface.

2.1 LGS Objective optical design

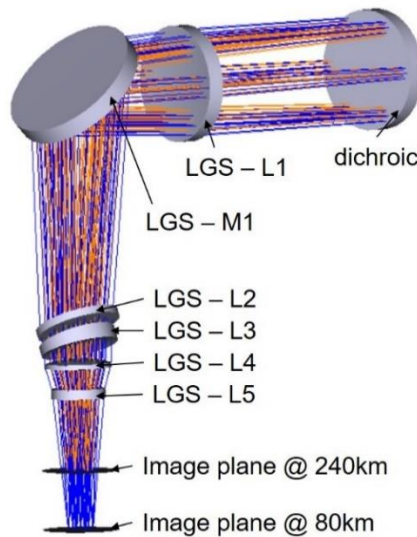


Figure 2: optical design of the LGS Objective.

The LGS light propagated through mirrors M6, M7, M8 (DM) and M9 (DM) is transmitted by the LGS Dichroic, which is located closed to a pupil plane, and is focused by the LGS Objective to create an image of the 6 LGSs for the LGS WFS sub-system.

The general specifications of the LGS Objective are reported in the next table.

Item	Value
Operating wavelength	0.589 μm
LGS range to be re-imaged	80 – 240 km
Exit focal ratio	F/5
Exit pupil distance	Infinity
LGS constellation maximum angular diameter	< 120 arcsec

Table 3. Main Path Optics general specifications.

The LGS Objective is designed to focus the LGS images in the altitude working range 84 - 240 km. This range covers from Zenith, where the sodium layer mean altitude is about 90km to the maximum zenith angle for AO observations, 70° . The output focal ratio of F/5 allows reasonable motion of the exit image plane, as a function of Zenith distance variation during the observation.

The 6 LGSs are supposed to be launched from the edge of the primary mirror and thus they rotate as the Zenith angle of observation. Their image plane shifts along the optical axis due to the variation of the mean distance of the LGS from the telescope, as $h_{Na}/\cos(\theta)$, where $h_{Na} \approx 90$ km is the Sodium layer mean altitude above the ground.

The LGS Objective, shown in Figure 2, consists of five lenses and a flat mirror. The baseline material for all refractive elements is optical glass (BK7, S-BSL7 or equivalent glass) but since the light is monochromatic, any suitable glass can be used. A part of the first lens LGS-L1, all other lenses are placed after the folding mirror, so that the LGS WFS sub-system is mounted in gravity invariant configuration. The next table shows the prescription data of the optical elements in the LGS Objective. Detailed performance and tolerance analysis of the LGS Objective are shown in section 3.

ID	Diameter [mm]	Thickness [mm]	Radius [mm]	Conic constant [1]	Tilt /degrees)
LGS-L1	620	61	(cx) -1180 (cx) -2220	-2.7 -0.8	-4
LGS-M1	620	-	flat	-	
LGS-L2	400	41	flat flat		-24 5
LGS-L3	390	-	(cx) -1330 (cx) -1340	-2.78 -0.8	-15
LGS-L4	360	21	(cx) 450 (cv) -1200	-1.258 -1.007	2
LGS-L5	320	48	(cv) 960 (cx) 515	-0.37 0	1

Table 4. Prescription data of optical elements in the LGS Objective. When two values are contained inside a single row, they refer to the front and rear surface of the optical element.

3. ANALYSIS REPORT

We present in this section the foreseen performance of the MPO and the LGS Objective. Besides the expected performance for the WFE for both of the science channel and the LGS channel, a detailed explanation of the geometric distortion at the instruments exit ports is given, since this requirement is one of most important science drivers for MICADO.

3.1 Main Path Optics wavefront error

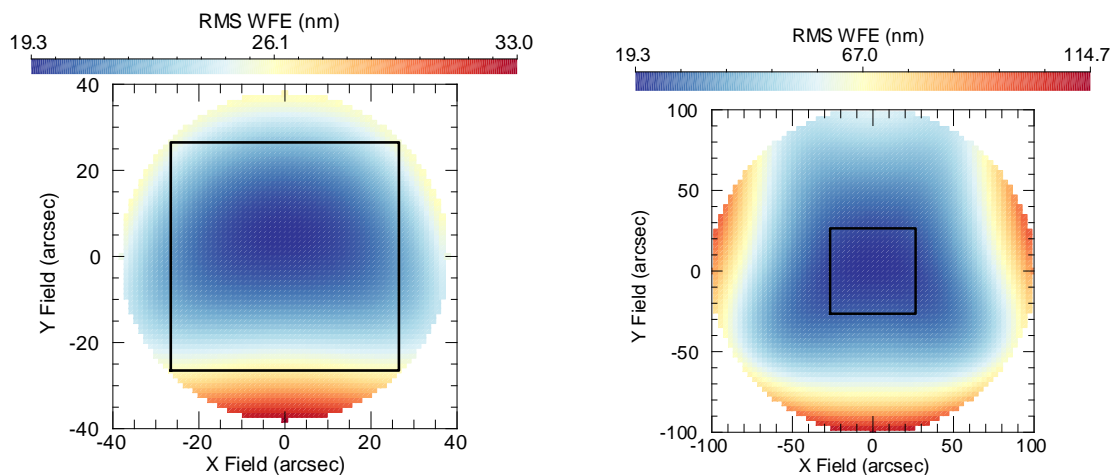


Figure 3. Left: WFE at the exit port of MAORY for the nominal optical design. The MICADO FoV of 53×53 arcsec² is enclosed in the 75 arcsec diameter circle; right: WFE at the exit port of MAORY for the nominal optical design. The NGS patrol FoV is enclosed between the MICADO FoV of 53×53 arcsec² and a 200 arcsec diameter circle.

The RMS WFE at the exit focal plane of the Main Path Optics, for the baseline design described in section 2, is shown in Figure 3 left for MICADO science FoV and in Figure 3 right for the technical FoV.

3.2 Geometric distortion

Geometric distortions from the MPO are asymmetric. As the imaged sky rotates with respect to the optics during an exposure, the PSF of a point-like source on the exit focal plane follows a trajectory, which may be described as an arc of a circle, with small perturbations due to the geometric distortions from the optics. Field derotation applied by MICADO only compensates for the circular part of the trajectory. The residual deviations from a circular trajectory have different effects, which are described below.

PSF blur due to geometric distortion

On the MICADO FoV, the residual motion of the PSF, when integrated over a finite exposure time, translates into PSF blur. The requirement has been calculated as following:

- T = Maximum integration time for narrow band astrometric observations ≈ 120 s
- A = Maximum derotator angular velocity $\approx 13.7 \times (1/\cos(80^\circ)) \approx 79$ arcsec/s
- $T \times A \approx 2.6^\circ$
- During this rotation, the FWHM of the long-exposure PSF due to the MAORY optics should not increase by more than 1/10 of its nominal value.
- For wavelength $\lambda = 1 \mu\text{m}$, the amount of distortion shall be $< 8 \mu\text{m}$ at the MAORY exit focal plane on the MICADO FoV ($F/17.7$ focal ratio).

The requirement above has been used in the optical design optimization and is fulfilled by design, as is shown in Figure 4 left.

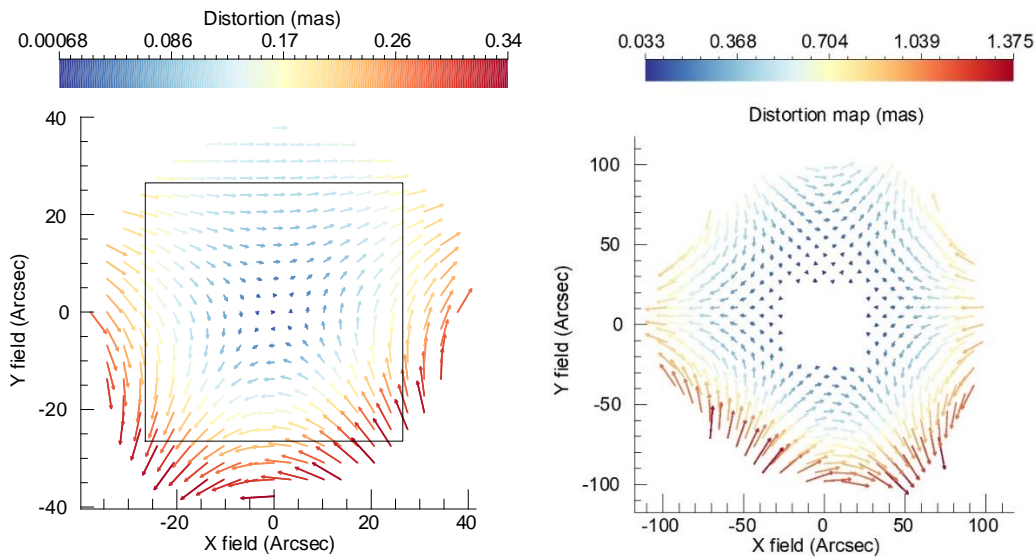


Figure 4. Left: Star centroids movement for a single astrometric image in the circle containing the MICADO FoV (black square). The longest integration time for a single astrometric image is 120 seconds, corresponding to 2.6° field rotation. Right: Star centroids movement for a single astrometric image in the circle containing the technical FoV. The longest integration time for a single astrometric image is 120 seconds, corresponding to 2.6° field rotation.

Effect of geometric distortion on NGS patrol FoV

Positioning errors of the NGS WFS probes are propagated by the MCAO system, producing science field warping effects. If the NGS WFS probes are positioned on the respective stars at the beginning of a sequence of astrometric exposures, during the integration time the stars will drift with respect to the probes, because of the non-rotational part of the geometric distortion itself. Since only 3 NGSs are used, the maximum order of the distortion is quadratic. The induced distortion in

the MICADO FoV can be divided in global tip-tilt equal to the mean value of the NGSs and the field stretch that is proportional to the distance of the star from the center. The very tight requirements for the PSF blur in the MICADO FoV described in the previous sub-section make this requirement not to have a significant impact in the optical design.

Science field warping due to geometric distortion

In two different astrometric exposures, the images of a given source in the MICADO FoV are in slightly different positions, because of the non-central-symmetric distortion pattern. The typical calibration procedure adopted in astrometric observations with MICADO is that any two astrometric images are transformed onto each other by an astrometric transformation (e.g. polynomial transformation of n-th order), using field sources to determine the coefficients of the transformation. This implies that “low-order” distortions (of order $\leq n$ in the example adopted here) are corrected on the data themselves, while “high-order” distortions need to be small enough, in order to avoid complex calibration procedures based on look-up tables.

In order to analyze this effect, a regular grid of stars on the MICADO FoV has been used to evaluate the astrometric residual error. Let (X_{inp}, Y_{inp}) be the initial coordinates of the stars centroids, (X_o, Y_o) the coordinates of the stars centroids for a given FoV rotation angle, (X, Y) the corrected stars centroids according to a n-th order polynomial transformation of the form:

$$X = \sum_{i,j} Kx_{i,j} \cdot X_o^i \cdot Y_o^j$$

$$Y = \sum_{i,j} Ky_{i,j} \cdot X_o^i \cdot Y_o^j$$

Typical order of transformation is $n = 3, 4, 5$. The final error in the position is the standard deviation computed as the quadratic sum of the X and Y errors. Figure 5 shows the residual errors vs. field rotation angles; for each angle, a single astrometric exposure has been assumed with exposure time of 120 seconds. Residual errors have been computed for an astrometric transformation of order $n=3$. The errors are $< 1 \mu\text{as}$ for all rotation angles, well within the requirement.

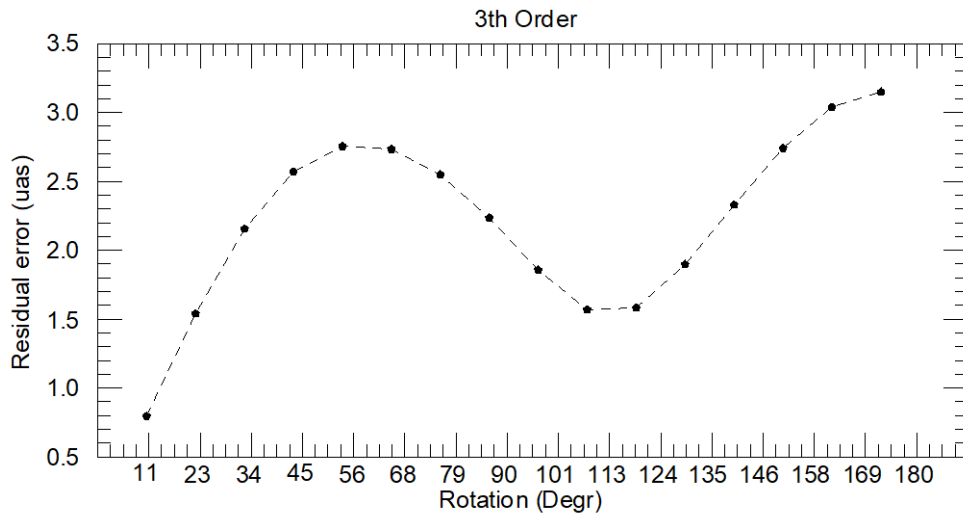


Figure 5. RMS residual distortion after 3rd order polynomial transformation over the MICADO FoV.

3.3 Main Path Optics exit pupil quality

The optical quality of the exit pupil, as it appears from the NGS WFS or the instrument point of view, has been tested by a paraxial lens placed after the relay. In the case of the NGS WFS, the pupil image is produced collecting the rays over a FoV of a few arcsec, which may be positioned anywhere on the full NGS patrol FoV (200 arcsec diameter). In the case of MICADO, the pupil image is produced collecting the rays over the MICADO FoV. The RMS radius of the pupil blur is

- 1/2000 pupil diameter for the NGS WFS, at any position in the NGS patrol FoV;
- 1/1000 pupil diameter for MICADO.

3.4 Main Path Optics deformable mirror conjugates

The post-focal DMs are conjugated to these ranges from the telescope entrance pupil:

- $H = 15000 \text{ m} \pm 230 \text{ m}$
- $H = 4500 \text{ m} \pm 170 \text{ m}$.

The quoted “errors” or “mis-conjugations” are due to the small tilt of the DMs with respect to the optical beam. Because of this mis-conjugation, an actuator at the edge of the DM is seen from the nominal conjugated layer under an angle < 200 arcsec (the NGS patrol FoV), which corresponds to a projected blur diameter of

- $4.4 \cdot 10^{-4} \text{ rad} \times 226 \text{ m} \approx 0.22 \text{ m}$, on the upper DM
- $4.4 \cdot 10^{-4} \text{ rad} \times 171 \text{ m} \approx 0.17 \text{ m}$, on the lower DM.

In any case, the blur diameter is in the order of 1/10 of projected inter-actuator spacing, which is considered as acceptable.

3.5 Main Path Optics simplified thermal analysis

A preliminary thermal analysis of the Main Path Optics has been carried out, considering the following assumptions:

- The positions of the optical elements change accordingly to temperature following the thermal contraction/dilation of a steel bench (CTE = 12 ppm/°C);
- Mirrors are made of “zero” expansion ceramics material (e.g. Schott Zerodur or similar); a CTE = 0.1 ppm/°C has been considered (Zerodur Expansion Class 2);
- Process is isothermal;
- The telescope focus has been used as compensator.

The thermal analysis has been carried out for a temperature range $T = 5^\circ\text{C} - 15^\circ\text{C}$.

Considering the entire system as a single configuration with a fixed temperature, multiple environments have been defined within the single configuration. The temperature range of the environments within a single configuration is $\pm 3^\circ\text{C}$. The main aberration due to the thermal change is astigmatism (Zernike mode Z6) and the effect is negligible.

At the time of the writing a more accurate thermo-elastic analysis, by means of FEM analysis on the mechanical structure, is being carried on in order to better evaluate the possible impact on the PFR performance.

3.6 LGS Objective wavefront error

The performance of the LGS Objective is shown in the next figures. Figure 6 shows the WFE vs. Zenith angle (after removal of tip-tilt and focus). The variation of wavefront with Zenith angle is very slow. The calibration procedure to remove these quasi-static aberrations from the LGS measurements might be based on temporal filtering of the LGS WFS measurements. Figure 7 shows the variation of residual WFE vs. Zenith angle (after removal of tip-tilt and focus), assuming that the average wavefront computed over the last 4 minutes (that is a degree of variation of the Zenith angle at the maximum rate) is subtracted from the wavefront at the previous angle. The residual WFE is indeed very small, $< 10 \text{ nm}$ for all possible Zenith angles.

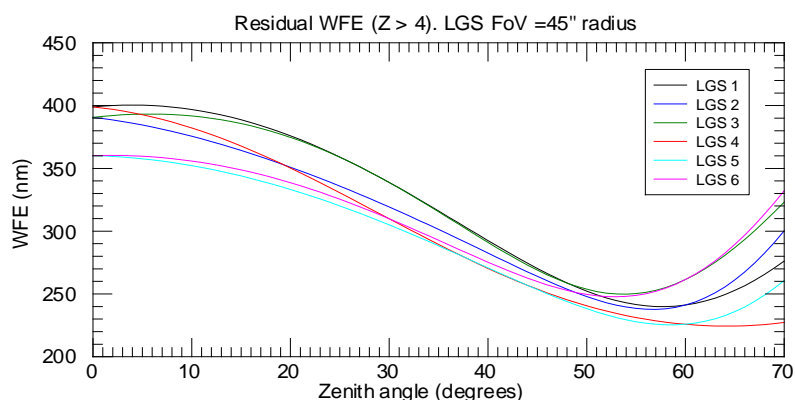


Figure 6. Residual WFE at the LGS Objective image plane (after removal of tip-tilt and focus) as a function of Zenith angle. The 6 curves correspond to an equal number of LGS, symmetrically arranged over a 45 arcsec radius FoV.

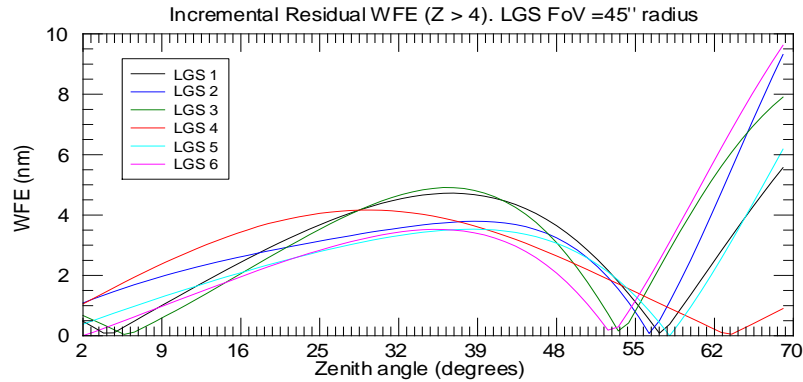


Figure 7. Variation of the residual WFE at the LGS Objective image plane (after removal of tip-tilt and focus) as a function of Zenith angle. The temporal average of the last 4 minutes is removed from the wavefront at each Zenith angle. The telescope tracks one degree every 4 minutes. The 6 curves correspond to an equal number of LGS, symmetrically arranged over a 45 arcsec radius FoV.

3.7 Tolerance analysis

The method used to estimate tolerances takes care of compensation of errors during assembly/alignment procedure and uses a Root-Sum-Square (RSS) approach to combine independent error contributions. The sensitivity analysis on system performance considers each tolerance individually and, once a merit function is defined, the errors are combined by RSS to find the net effect of all the tolerances on the system. This method assumes that errors introduced by a given tolerance are statistically uncorrelated and allows to identify parameters which are highly sensitive to certain errors, such as surface curvature radii or decenters.

The sensitivities related only to available Degree-Of-Freedom (DOF) can be used during the alignment phase of the instrument since the worst offenders to system performance are also the best set of compensators for required adjustments. There are two requirements that limit the allowable changes of opto-mechanical parameters: the FoV-averaged RMS WFE and the geometric distortion.

Considering the RMS WFE, the goal was to maintain the maximum WFE on all the MICADO FoV below the diffraction limit @ 1 μ m wavelength (70nm RMS) while regarding the geometric distortion the goal was to remain below the requirements of Table 1, since the nominal design has a better performance. The tolerance analysis has been broken down into 2 blocks that consider different error sources of the optical elements.

Block 1 is the manufacturing tolerance and can be split into 2 sub blocks: curvature radii and low order surface irregularities ($4 < z < 11$) and high order surface irregularities. Precision optics are required to maintain the WFE degradation below the requirements for the first sub block. Moreover a partial compensation can be done re-optimizing the optical design once the real parameters are measured after the manufacturing. High order surface irregularities affect mainly astrometry, since the PFR does not rotate as the sky. In particular M11, the mirror closest to the focal plane is the most critical element.

Block 2 is the mechanical tolerance and set the precision and stability of the mounts and alignment stages. Regarding the assembly precision, the laser tracker precision is sufficient for our requirements and the high precision commercial stages can fulfil our needs regarding the repeatability.

Alignment concept

The MPO alignment plan is foreseen to be carried on in two steps:

1. Optics, entrance focal plane (where to put optical fibers) and exit focal plane (where to put cameras and WFSs) are positioned with laser tracker precision;
2. The final alignment.

The sensitivity analysis identified the worst offender DOF that are used as active compensators (Figure 8); they should work in combination with the metrology system that provides the necessary information to change the optical path according to estimated misalignments. A Monte Carlo simulation has been carried out simulating the entire procedure. For each case it is assumed to use some sources at the entrance focal plane and measure both positions and WFs at the exit focal plane. Zernike coefficients and distortion values are target values of the merit function of the nominal design. The optimization is done using the damped least squares algorithm and the compensators as variables. The perturbed degree

of freedom of compensators are the mis-alignments that generated the measured Zernike coefficients and distortion values and that should be compensated. This solution, called Reverse Optimization (RO) is described in detail in [8].

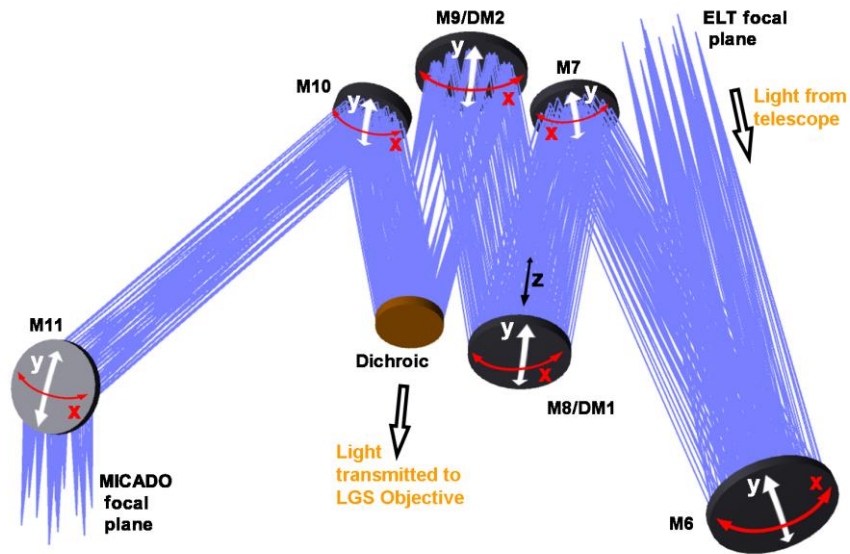


Figure 8. MAORY MPO and its DOF compensators. Tilts on local x and y axes are necessary compensators to achieve diffraction limited optical quality during the alignment (plus one mirror axial distance Z). M11 Tilts are additional compensator to achieve the requirement on the geometrical distortion.

The results of the RO are that the mean residual WFE in the MICADO FoV is few nanometers bigger than the nominal design. Regarding the geometrical distortion, the error is about 1mas at the edge of the MICADO field. We are currently adding to this procedure the possible errors in the measurement of the spots centroids and WF that we expect to have in the real system during the alignment phase in the lab and during the commissioning at the telescope, in order to give requirements to the Calibration Unit of MAORY.

4. CONCLUSIONS

We presented the current optical design of the PFR of MAORY, which is Phase B and is expected to have the Preliminary Design Review at late spring 2019. We showed that the requirements concerning the residual WFE and the geometrical distortion can be achieved together with the other requirements. Due to the non-center symmetric pattern of the distortion even aspheric terms in one of the MPO mirror surface (M10) are necessary but a preliminary consultation with optics manufacturing companies result that all MOARY optics are feasible. At the time of the writing, a detailed investigation on the thermo-elastic behaviors of the optical bench and support structure of MAORY is being carried on. This could affect the analysis regarding the alignment concept, causing the introduction of more compensators to actively adjust the positioning of the optics. The next step regarding the optical design is the refinement of some crucial parameters, as the DM conjugation altitude or the number of actuators that will be confirmed in the next months.

REFERENCES

[1] Diolaiti, E., Ciliegi, P., Abicca, R., Agapito, G., Arcidiacono, C., Baruffolo, A., Bellazzini, M., Biliotti, V., Bonaglia, M., Bregoli, G., Briguglio, R., Brissaud, O., Busoni, L., Carbonaro, L., Carlotti, A., Cascone, E., Correia, J.-J., Cortecchia, F., Cosentino, G., De Caprio, V., de Pascale, M., De Rosa, A., Del Vecchio, C.,

- Delboulbé, A., Di Rico, G., Esposito, S., Fantinel, D., Feautrier, P., Felini, C., Ferruzzi, D., Fini, L., Fiorentino, G., Foppiani, I., Ghigo, M., Giordano, C., Giro, E., Gluck, L., Hénault, F., Jocu, L., Kerber, F., La Penna, P., Lafrasse, S., Lauria, M., le Coarer, E., Le Louarn, M., Lombini, M., Magnard, Y., Maiorano, E., Mannucci, F., Mapelli, M., Marchetti, E., Maurel, D., Michaud, L., Morgante, G., Moulin, T., Oberti, S., Pareschi, G., Patti, M., Puglisi, A., Rabou, P., Ragazzoni, R., Ramsay, S., Riccardi, A., Ricciardi, S., Riva, M., Rochat, S., Roussel, F., Roux, A., Salasnich, B., Saracco, P., Schreiber, L., Spavone, M., Stadler, E., Sztefek, M.-H., Ventura, N., Véronaud, C., Xompero, M., Fontana, A., Zerbi, F. M., "MAORY: adaptive optics module for the E-ELT", *proceedings of the SPIE*, Volume 9909, id. 99092D 7 pp. (2016).
- [2] Tamai, R., Cerasuolo, M., González, J. C., Koehler, B., Tuti, M., "The E-ELT program status", *Proceedings of the SPIE*, Volume 9906, id. 99060W 13 pp. (2016).
- [3] Davies, R., Schubert, J., Hartl, M., Alves, J., Clénet, Y., Lang-Bardl, F., Nicklas, H., Pott, J.-U., Ragazzoni, R., Tolstoy, E., Agocs, T., Anwand-Heerwart, H., Barboza, S., Baudoz, P., Bender, R., Bizenberger, P., Boccaletti, A., Boland, W., Bonifacio, P., Briegel, F., Buey, T., Chapron, F., Cohen, M., Czoske, O., Dreizler, S., Falomo, R., Feautrier, P., Förster Schreiber, N., Gendron, E., Genzel, R., Glück, M., Gratadour, D., Greimel, R., Grupp, F., Häuser, M., Haug, M., Hennawi, J., Hess, H. J., Hörmann, V., Hofferbert, R., Hopp, U., Hubert, Z., Ives, D., Kausch, W., Kerber, F., Kravcar, H., Kuijken, K., Lang-Bardl, F., Leitzinger, M., Leschinski, K., Massari, D., Mei, S., Merlin, F., Mohr, L., Monna, A., Müller, F., Navarro, R., Plattner, M., Przybilla, N., Ramlau, R., Ramsay, S., Ratzka, T., Rhode, P., Richter, J., Rix, H.-W., Rodeghiero, G., Rohloff, R.-R., Rousset, G., Ruddenklau, R., Schaffenroth, V., Schlichter, J., Sevin, A., Stuik, R., Sturm, E., Thomas, J., Tromp, N., Turatto, M., Verdoes-Kleijn, G., Vidal, F., Wagner, R., Wegner, M., Zeilinger, W., Ziegler, B., Zins, G., "MICADO: first light imager for the E-ELT", *Proceedings of the SPIE*, Volume 9908, id. 99081Z 12 pp. (2016)
- [4] Bonaccini Calia, D., Feng, Y., Hackenberg, W., Holzöhner, R., Taylor, L., Lewis, S., "Laser Development for Sodium Laser Guide Stars at ESO" *The Messenger*, 139 (2010).
- [5] Rigaut, F., and Gendron E., "Tilt anisoplanatism and PSF retrieval in LGS MCAO using a predictive controller", *A&A*, 261,, pp.677-684 (1992).
- [6] Rodeghiero, G., Pott, J.-U., Bizenberger, P., "Study of the impact of E-ELT and MICADO distortion and wavefront errors residuals on the MICADO astrometric observations", *Proceedings of the SPIE*, Volume 9908, id. 99089E 18 pp. (2016).
- [7] Patti, M., Lombini, M., Magrin, D., Diolaiti, E., Cortecchia, F., Arcidiacono, C., Ciliegini P., Feautrier, P., "MAORY tolerance analysis", this conference, paper number 10690-78 (2018).
- [8] Patti, M., Lombini, M., Magrin, D., Diolaiti, E., Cortecchia, F., Arcidiacono, C., Ciliegi P., Feautrier, P., "Precise alignment method for MAORY", *SPIE Astronomical Telescopes + Instrumentation 2018*, paper number 10705-14 (2018)